Viability of wall-embedded tag antenna for ultra-wideband real-time suitcase localisation

Andela Zaric[1], Valter S. Matos[1], Jorge R. Costa[1,2], Carlos A. Fernandes[1]

[1]Instituto de Telecomunicações, Instituto Superior Técnico – Universidade Técnica de Lisboa (IST-UTL), Lisboa 1049-001, Portugal

[2]Departamento de Ciências e Tecnologias da Informação, Instituto Universitário de Lisboa (ISCTE-IUL), Lisboa 1649-026, Portugal

E-mail: azaric@lx.it.pt

Abstract: Viability of a conformal single-layer monopole antenna is studied for a wall-embedded tag in an ultra-wideband (UWB) suitcase localisation application based on impulse radio UWB. The performance of the embedded antenna is simulated and confirmed experimentally in real-time localisation (RTL) experiments carried out in a cluttered laboratory environment. Evaluation in the main planes shows average suitcase positioning error around 8 cm for worst-case conditions. RTL tests are made when the suitcase is empty, when it is filled with common travelling items and also when it is shadowed by a second suitcase. A vector network analyser-based measurement set-up is used for target localisation error evaluation. Additionally, the same tests are repeated using portable commercial time-domain transceivers with similar results.

1 Introduction

Wireless indoor localisation systems have been raising a lot of interest, and numerous studies have yielded quite a few candidate systems [1]. Most of the spread radio frequency (RF) indoor localisation systems are based on wireless local area network, offering several metre to 1 m precision with numerous base stations deployed inside the indoor space [1–3]. The newest localisation technologies are based on radio frequency identification (RFID) and ultra-wideband (UWB), each type with its specific strong and weak points. RFID enables identification of objects with 1–2 m precision within up to 300 m range using active tags [3]. On the other hand, impulse radio UWB (IR-UWB)-based systems provide centimetre precision [4–6] even with passive tags [7]. However, indoor range for active UWB tags reaches only up to 10 m limited by energy regulations [8] whereas for passive tags it is much shorter (up to 1 m).

In logistic localisation systems, RFID baggage tagging and tracking is already implemented in a few airports worldwide [9]. Usually, the RFID tags are attached to the classical barcode strap wrapped around the baggage handle. An alternative was studied in [9], where the RFID tag is embedded into the wall of hard-shell suitcases during fabrication. This protects it from harsh luggage handling and enables its reprogramming at the airport at each new journey. Laboratory experiments have shown 100% RFID reading score with our tag in typical travel conditions sliding on a conveyor belt [9].

Building upon the previous experience, this paper proposes extending the embedded RFID tag concept from [9] by adding the possibility of IR-based suitcase localisation,

using a suitable co-designed IR-UWB antenna. The antenna is designed taking into account the influence of the embedding hard suitcase wall shape and dielectric material to ensure reasonable preservation of the impulse shape for all solid angle, thus favouring precise ranging estimation irrespective of suitcase orientation. Localisation performance is evaluated by simulation and experiments in a real system with empty, filled and shadowed suitcase. So, the objective of the present work is to study the suitcase localisation accuracy and the tag detection reliability for all solid angle and all suitcase orientations using a conformal wall-embedded IR-UWB antenna. Simulation results and tests performed with a real IR-UWB system show very good performance, validating the concept.

The IR-UWB antenna tag and its performance are described in Section 2. A real-time locating system (RTLS) testbed developed at the Laboratory is used to demonstrate the achievable suitcase localisation accuracy in Section 3. Furthermore, IR-UWB tag-to-sensor distance effect is evaluated, as well as suitcase orientation, content and shadowing influence. In Section 4, conclusions are drawn.

2 IR-UWB tag antenna

Previous experience [9] has shown that the best angular detection coverage for an RFID tag is achieved if the tag is conformal and embedded into the suitcase lid close to the rounded top corner. Hence, similar position is maintained here in order to ensure best omnidirectional coverage in all planes using an IR-UWB monopole-like antenna. This means that this antenna must be conformal with the lid shape near the rounded top corner.

To embed the antenna into the suitcase wall during the injection moulding process, it must be very thin and structurally robust enough to withstand the embedding process. Moreover, the antenna has to preserve the pulse shape in the whole solid angle to offer reliable localisation capabilities. The proposed configuration derives from the classical monopole antenna (Fig. 1) and it is co-designed to fulfil the above requirements. The uniplanar configuration enables using a very thin flexible substrate, similar to [10, 11]; however, these papers do not address the antenna localisation performance or the influence of attached objects.

The main radiating element of Fig. 1 is a gapped circular loop fed by a coplanar waveguide line. Unlike the traditional monopole antennas that tend to present well-defined linear polarisation – an handicap for arbitrary orientation tag detection – the proposed antenna with its loop configuration is less sensitive to polarisation favouring good signal reception from any direction and for any orientation of a linearly or circularly polarised receiving antenna. Antenna dimensions as denoted in Fig. 1 can be found in Table 1. The coplanar waveguide line is linearly tapered out towards the loop to match the antenna impedance to the 50 Ω impedance of the coaxial connector at the bottom of the antenna. The rounded corner of the suitcase lid and the need to embed the antenna in the suitcase wall has motivated the use of a 50 μm thick flexible polyester laminate [12] substrate with permittivity $\varepsilon_r = 2.1$ and loss tangent 0.002.

Since the whole suitcase is too large to be included in the antenna simulation model, only a representative 80 mm × 14 mm bent dielectric sheet (permittivity $\varepsilon_r = 2.4$, loss tangent 0.003 and thickness 2.8 mm) is placed against the antenna, as shown in Fig. 1b. Simulations have shown that the size of the dielectric used to represent the suitcase wall does not influence significantly the antenna results, beyond the used dimensions. The main influence comes, however, from the wall dielectric properties, its curved shape and its proximity to the antenna itself. The bending curvature radius for both the dielectric sheet and the tag antenna is 7 cm corresponding to the curvature of the suitcase in Fig. 1c

at the tag antenna position. The xyz coordinate system shown in Fig. 1b is associated with the antenna and it will be used onwards for all the presented results. The antenna and suitcase models (Fig. 1b) were simulated using CST time-domain solver [13].

Fig. 2a presents the simulated and measured voltage standing wave ratio (VSWR) for the bent tag antenna with attached dielectric sheet. Measured curve compares well with simulations. Good impedance matching is obtained over the entire band from 3.1 to 5.1 GHz, denoted with the grey shadowed area in the same figure. Apart from the usual monopole parameters, the specific parameters from this configuration that have most influence on the antenna VSWR are d and Θ. Its effect is shown in Fig. 2. Parameter d influences the resonance frequency whereas parameter Θ their depth and width.

Although not shown, several tests were also performed for different antenna bending according to different antenna distances to the rounded corner of the suitcase lid (from antenna not bent to entirely bent), with little deviation from the presented curve. This means that the same antenna can be used with different suitcase dimensions and different positions if necessary.

Fig. 3 presents the simulated realised gain and total efficiency of the used antenna. The observed behaviour is typical for monopole-like UWB antennas, that is, the efficiency is high and gain is almost constant throughout the entire band with average value of 3 dBi.

For accurate range determination using IR-UWB, it is crucial that the antenna preserves the transmitted (or received) pulse shape. Pulse distortion introduced by the antennas contributes to erroneous ranging results, given that range is computed from the impulse time of arrival (ToA) which is determined either by maximum peak detection or rising edge detection. Therefore, if the received pulse is significantly distorted, the ToA estimate will not be accurate. A good figure of merit to characterise the pulse distortion is pulse fidelity [14]; it provides a measure of correlation between the received pulse and the transmitted one. In other words, fidelity shows the level of agreement
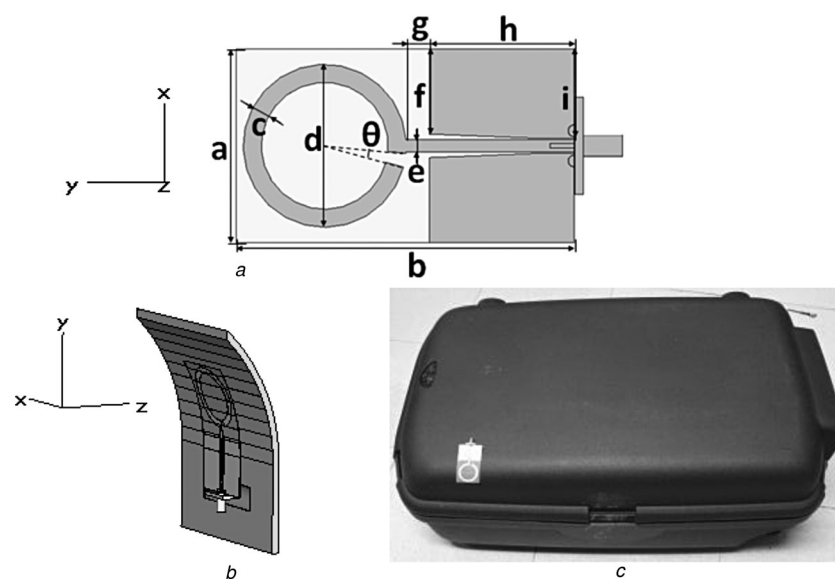

Fig. 1 *UWB tag antenna configuration*

a Planar model with dimensions indicated in Table 1
b Bent tag antenna and dielectric plate simulation model
c Placement in the suitcase (Note: figure is demonstrative – the tag antenna is actually placed inside the suitcase at the same position)
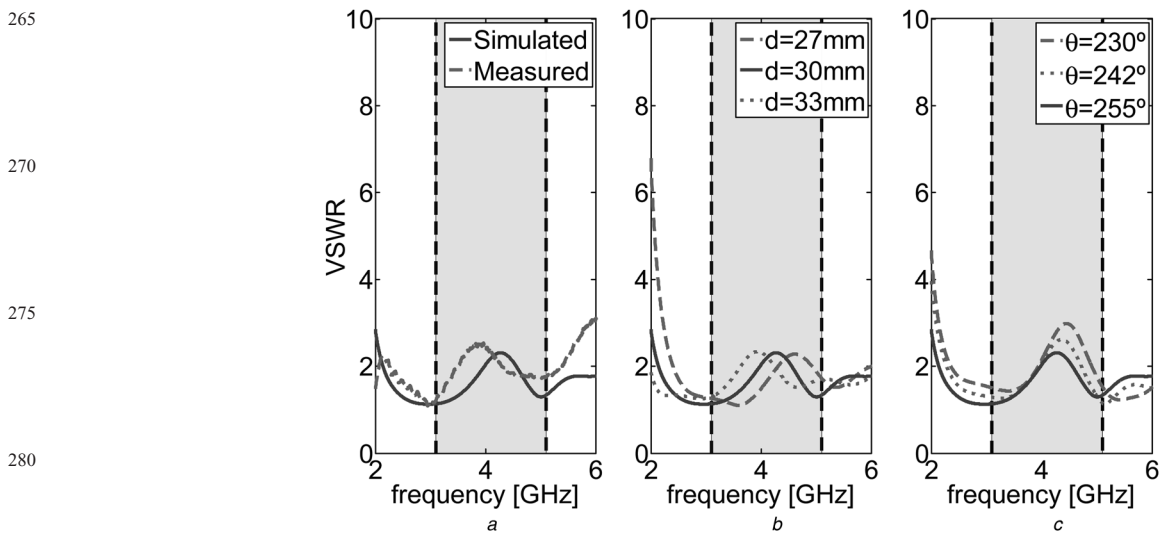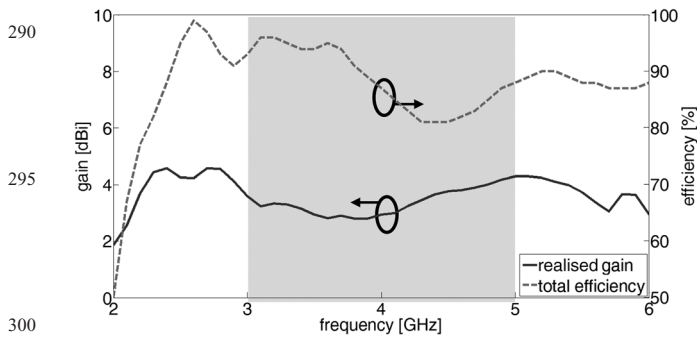
Fig. 2 *Simulated and measured VSWR*

a Simulated and measured VSWR for the fabricated prototype
b Simulated VSWR for three different values of parameter *d* (outer diameter of the loop)
c Simulated VSWR for three different values of parameter Θ (angular position of the loop gap); (grey shadowed area denotes the used frequency band)

Q1

Q2 **Fig. 3** *Simulated realised gain (full blue line) and total efficiency (dashed red line); (grey shadowed area denotes the used frequency band)*

between the transmitted and received pulses, and ideally its value should be 100% corresponding to two identical pulses. In fact, pulse fidelity integrates in a consistent way
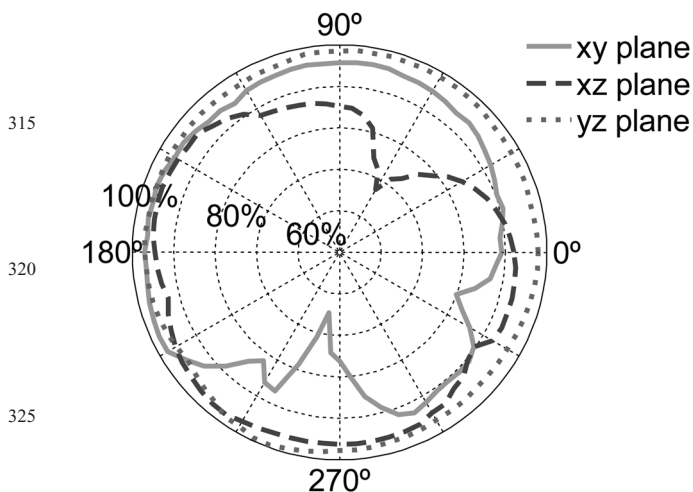

Fig. 4 *Measured angular dependence of pulse fidelity for xz-, yz- and xy-planes*

all the required angular information about the antenna radiation pattern and phase centre against frequency, providing a quantitative measure of pulse shape preservation. Since high fidelity is very important for accurate range detection, it is also important to quantify the fidelity in all angular directions when the antenna is integrated with the object, especially for a suitcase detection and localisation application where the suitcase can be in any number of orientations. Fig. 4 shows the angular variation of measured pulse fidelities for the embedded tag antenna in the three principal planes. This is calculated using the procedure described in [15] for a test Gaussian pulse complying with FCC indoor mask [8] and centred in the 3.1–5.1 GHz band

$$u(t) = \cos(2\pi f_c t) \exp\left[-2\pi\left(\frac{t}{\tau}\right)^2\right] \qquad (1)$$

with central frequency $f_c = 4.1$ GHz and Gaussian width $\tau = 0.95$ ns. As seen in Fig. 4, pulse fidelity performance changes with the scan plane and with the pulse angle of arrival. Fidelity for the *yz*-plane is always close to 100%, meaning that the pulse is almost undistorted by the antenna. In the other two planes, *xy* and *xz*, there are angular regions where the fidelity value is lower than 80%, anticipating slightly lower ranging performance than for the *yz*-plane, and consequently, possible worse localisation accuracy. A quantified analysis of the ranging error is presented ahead.

3 Experimental performance evaluation

3.1 RTLS platform

A two-dimensional UWB RTL platform was developed at Instituto de Telecomunicações to serve as a visual tool to quickly test new UWB antennas and algorithms for localisation. It includes two basic modules controlled by a personal computer (PC): an optical position measurement system based on a web-camera; and a UWB range and position measurement system comprising a four-port VNA, three UWB sensor antennas and a control code running on
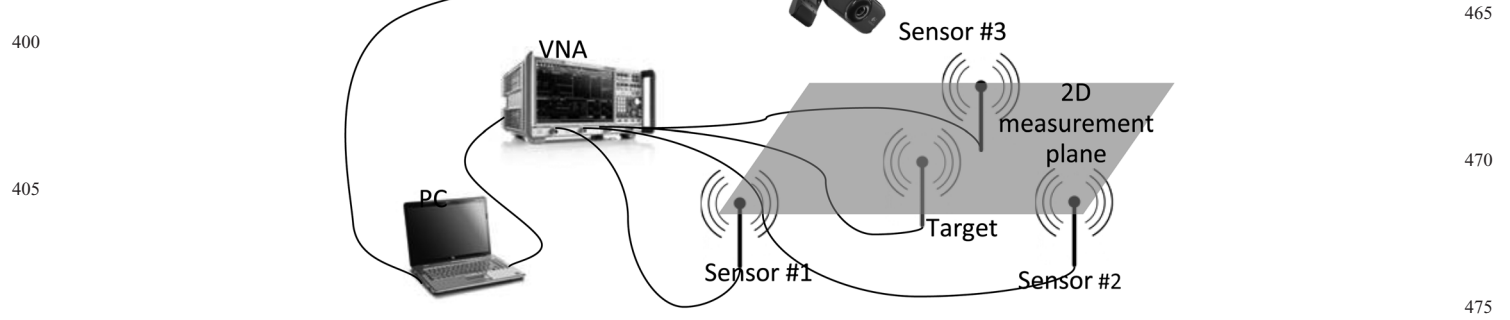
Fig. 5 *UWB RTL system schematics*

the PC, as seen in Fig. 5. The UWB estimated target position and the corresponding optically determined counterpart are marked on the image from the scenario acquired in real time and displayed on a large screen, providing immediate quantitative indication of the target position estimation error. The system can record and post-process the position and orientation history of the target along its travel path in the scenario.

The webcam is placed near the ceiling above the measurement area to minimise occlusion of the target antenna optical tracking pattern. After image perspective distortion calibration, the HD resolution of 1024×576 pixels offers 6 mm space resolution. The details of the image calibration and optical localisation algorithm are out of the scope of this paper. For the present work, three cavity-back spiral antennas with frequency stable unidirectional wideband LHCP radiation pattern are used as the fixed sensor antennas.

RF localisation requires the determination of the distance between each sensor antenna and the target antenna; this is obtained through frequency-domain S-scattering matrix post-processing as in [15]; so only a brief highlight of the procedure is given next. The control code logs automatically from the four-port VNA the scattering matrix elements between the sensor antennas (ports 1 to 3) and the target antenna (port 4), after full-port calibration. The $s4j$ $\{j = 1{:}3\}$ elements from the S-matrix are then multiplied by the spectrum of the test Gaussian pulse (1) and transformed into time domain to obtain the time domain received pulses. Pulse time of arrival (ToA) at each sensor antenna is calculated from this data using the highest peak detection algorithm, allowing the determination of the distance between antennas. Additionally, pulse fidelities are calculated for each of the received pulses.

A trilateration algorithm is implemented to calculate the target localisation from the measured distances. The ranging distances are represented as circles which intersect mutually. Owing to system errors, the circles never intersect on a single point, so the standard trilateration algorithm needs to be complemented with some criteria to select a solution out

from an ambiguity area [16]. In the present case, the chosen solution is the geometric centroid of this area.

3.2 Experimental results

The experimental set-up, as seen from the webcam, is shown in Fig. 6 (the axes are additionally inserted to give notion of the measurement area size). The set-up environment is a cluttered lab, which includes desks with metal legs and a row of metallic cabinets on the other two sides. Some of this furniture can be seen in Fig. 5. The three sensor antennas are mounted on tripods forming a triangle at the same height as the tag antenna in the suitcase. The suitcase (not shown in the image) with attached tag antenna is mounted on a foam pedestal in three different cases: with the antenna xy-plane, xz-plane and yz-plane parallel to the floor in each suitcase orientation (Fig. 6 shows some measured positions in xy-plane). The suitcase foam pedestal is randomly moved and rotated within the $3\,m \times 2\,m$ measurement area, covering about 150 points for each antenna measurement plane.

For clarity, the suitcase is not shown in Fig. 6, but instead some of its 150 positions acquired by the optical module are marked with green arrows. The tip of the arrow represents the tag location and it is linked through a black line to the corresponding estimated position (red dot marker) obtained from the UWB module. Thus, the line length corresponds to the magnitude of the localisation error in each case.
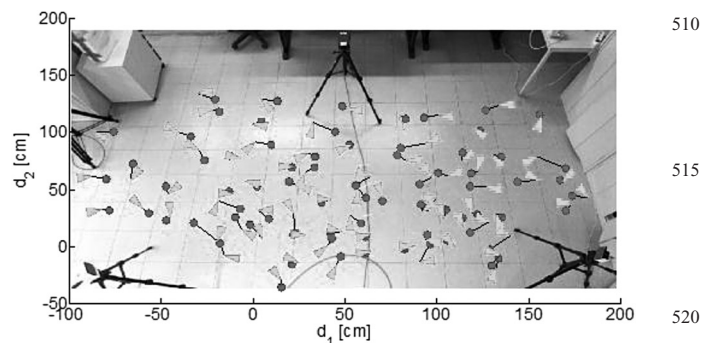

Fig. 6 *Measurement set-up and RTLS graphical output for measurements in xy-plane where the sensor antennas are mounted on tripods*

Tips of the green arrows denote the target position detected by the camera and the red dots the target position detected by the UWB RTL, black lines connect homologous markers, whereas the green arrows orientation denote suitcase angle orientation in the direction of y-axis of the tag antenna

Table 1 Dimensions of the UWB tag antenna[a]

parameter	a	b	c	d	e
value	32	56	3	30	2
parameter	F	g	h	i	Θ
value	14.058	3.837	24	14.8	10

[a]All dimensions in mm, except θ which is in degrees
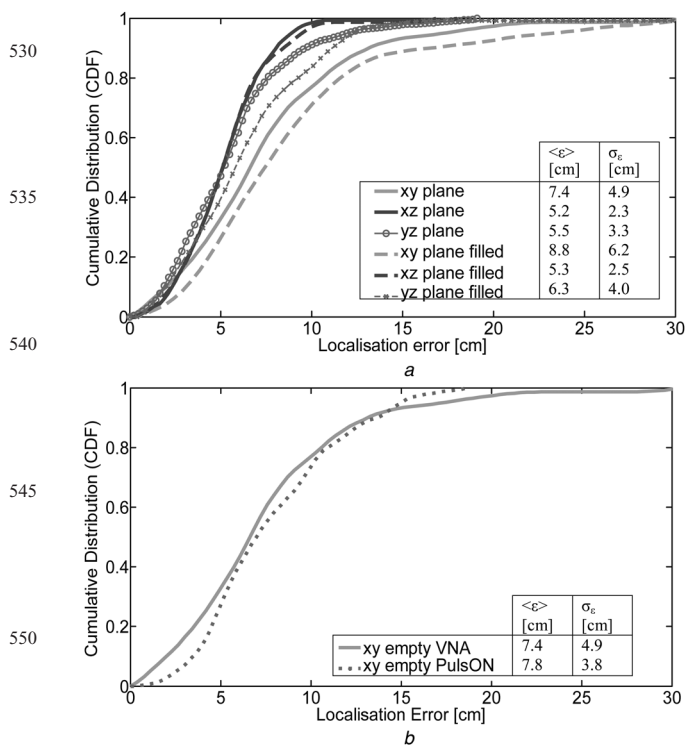
Fig. 7 *Localisation error cumulative distribution function*

a For all three antenna/suitcase planes, for empty and filled suitcase with travel items
b In the *xy*-plane, comparing VNA-based and direct time-domain measurements
Insets summarise corresponding average error and standard deviations

Additionally, the arrow orientation indicates the suitcase angle orientation obtained from the optical module, pointing in the direction of *y*-axis of the tag antenna itself. These measurements correspond to the tag antenna *xy*-plane case, attached to the empty suitcase. Fig. 6 shows small discrepancies between the assumed correct optical position and the position measured by the UWB module. These results are analysed in more detail next.

Fig. 7*a* shows the cumulative distribution function (CDF) of the localisation error for each of the three suitcase/antenna planes, both for the empty suitcase and when fully filled with usual travel items (clothes, shoes, books, cosmetics, tooth-paste, and so on), considering the whole dataset of measurements. For all three planes of the empty suitcase (solid line: light green, dark blue and red with circle markers in Fig. 7*a*), 90% of the measured points have localisation error smaller than 12.5 cm, whereas 80% of all points falls under 10 cm and have average positioning error value around 6 cm. This shows that despite the very reflective close environment, the accuracy of suitcase localisation is quite good for all orientations, enough for the present application. Furthermore, it shows that the filling of the suitcase does not influence significantly the localisation capabilities of the UWB tag antenna.

However, it is visible that localisation is slightly more accurate (lower standard deviation) in *xz*- and *yz*-planes than in the *xy*-plane. This can be explained by the fidelities presented in Fig. 7, where *xy*-plane has a slightly larger angular interval of fidelities below 80% than the other two curves. When the suitcase is filled with travel items (dashed lines in Fig. 7*a*), the accuracy in *xy*-plane (light green) and *yz*-plane (red line with cross marker) decreases slightly

whereas in *xz*-plane (dark blue) it remains almost equal to the empty case. In the latter case, gravity pulls down the suitcase contents away from the antenna, thus creating less shadow on it. Anyway, for all cases the average error and standard deviation show about 1 cm difference between empty and filled suitcase measurements, confirming that travel items have marginal influence on localisation accuracy for the selected antenna positioning in the suitcase. In comparison with the suitcase dimensions, these results are enough for its reliable localisation. In addition, similar measurements are repeated in *xz*-plane when the suitcase is shadowed by another one tightly placed side-by-side, hiding the tag antenna: only 2 cm increase in average positioning error is obtained, proving the concept and the adequacy of the proposed tag antenna even in this case. In other words, the described experiments show that the localisation capability of the UWB tag antenna are reliable when surrounded by materials with various dielectric properties from all sides (filling items inside suitcase and another suitcase in front) despite the very reflective environment. Similar measurements as the ones presented in Fig. 7*a* have also been performed using a commercial non-conformal rigid UWB antenna from SkyCross SMT-3TO10M-A [17]. The proposed flexible UWB tag has performed better in average by 66% than the commercial antenna showing the importance of conformal attachment for this application.

The used VNA-based post-processing ranging technique is certainly not practical for the end application. It remains to show that the proposed tag antenna performance and suitcase localisation results still hold when commercial time-domain transceivers are used instead of the VNA. For that, the previous test in the *xy*-plane of the empty suitcase is repeated with the VNA replaced by four commercial transceivers that operate directly in time domain with an IR protocol. PulsON® transceivers from Time Domain® [18] are connected directly to each of the sensor antennas and to the tag antenna inside the suitcase. Pulse spectrum is centred at 4.3 GHz and spans from 3.1 to 5.3 GHz with FCC indoor mask-compliant power density. The transceivers come with dedicated software to retrieve antenna ranging data only. The in-house developed platform is used to process this data and produce target localisation information and error data. The optical module from the UWB RTLS platform is used again to obtain the optical target position. Measurements with the PulsON® equipment are performed at 150 random points as before. The results are shown only for the *xy*-plane case, the most likely for a suitcase sliding on a conveyor belt. The corresponding CDF is presented in Fig. 7*b* as the red dotted curve and it is superimposed on corresponding VNA-based measurements. The curve and the summary in the inset show almost no difference between the two approaches, so it basically validates the procedure and the conclusions obtained from the VNA measurements. Unlike the VNA set-up, PulsON® measurements are not hassled by RF cables enabling ranging tests for larger distances between the sensor antenna and the suitcase embedded tag up to 5 m.

4 Conclusion

Viability of using a compact low-profile IR-UWB antenna for embedding into the wall of a travel suitcase is thoroughly tested in a localisation application. An in-house developed RTL system is used to evaluate the performance of the

suitcase-integrated antenna in its three main planes and correlation is found between pulse fidelity and the achieved ranging accuracy. Statistical analysis of a total of 1200 random suitcase locations and orientations inside the measurement area show that the average error is less than about 8 cm even when shaded by other suitcase, which is enough for this application. This demonstrates the antenna performance for all suitcase orientations, the adequacy of antenna placement in the suitcase and the feasibility of the suitcase UWB localisation concept. All tests were made in a cluttered environment with very close metallic cabinets and other reflecting furniture. A large class of suitcases use similar type of dielectric material and shape, so it is anticipated that these results can be considered applicable to a large number of practical cases.

Given the full solid angle antenna characterisation, similar results are expected for a full 3D scenario, which of course involves more sensor antennas. The concept can be extended for automotive industry, warehouse control, surveillance, and so on.

5 Acknowledgment

6 References

1   Hui, L., Darabi, H., Banerjee, P., Jing, L.: 'Survey of wireless indoor positioning techniques and systems', *IEEE Trans. Syst. Man Cybern. Part C: Appl. Rev.*, 2007, **37**, pp. 1067–1080

2   Shih-Hau, F., Tsung-Nan, L.: 'Principal component localization in indoor WLAN environments', *IEEE Trans. Mobile Comput.*, 2012, **11**, pp. 100–110

3   Shih-Hau, F., Tsung-Nan, L.: 'Cooperative multi-radio localization in heterogeneous wireless networks', *IEEE Trans. Wirel. Commun.*, 2010, **9**, pp. 1547–1551

4   Ni, L.M., Dian, Z., Souryal, M.R.: 'RFID-based localization and tracking technologies', *IEEE Wirel. Commun.*, 2011, **18**, pp. 45–51

5   Segura, M., Mut, V., Sisterna, C.: 'Ultra wideband indoor navigation system', *IET Radar Sonar Navig.*, 2012, **6**, pp. 402–411

6   Kuhn, M.J., Mahfouz, M.R., Zhang, C., Merkl, B.C., Fathy, A.E.: 'A system-level simulation framework for UWB localization', *IEEE Trans. Microw. Theory Tech.*, 2010, **58**, pp. 3527–3537

7   Gezici, S., *et al.*: 'Localization via ultra-wideband radios: a look at positioning aspects for future sensor networks', *IEEE Signal Process. Mag.*, 2005, **22**, pp. 70–84

8   FCC 02-48: 'Federal Communications Commission (FCC), first order and report: revision of part 15 of the commission's rules regarding UWB transmission systems', 22 April 2002

9   Medeiros, C.R., Costa, J.R., Fernandes, C.A.: 'Passive UHF RFID tag for airport suitcase tracking and identification', *IEEE Antennas Wirel. Propag. Lett.*, 2011, **10**, pp. 123–126

10 Nikolaou, S., Tentzeris, M.M., Papapolymerou, J.: 'Study of a conformal UWB elliptical monopole antenna on flexible organic substrate mounted on cylindrical surfaces'. IEEE 18th Int. Symp. Personal, Indoor and Mobile Radio Communications, PIMRC 2007, September 2007, Athens, Greece, pp. 1–4

11 Khaleel, H.R., Al-Rizzo, H.M., Rucker, D.G., Mohan, S.: 'A compact polyimide-based UWB antenna for flexible electronics', *IEEE Antennas Wirel. Propag. Lett.*, 2012, **11**, pp. 564–567

12 http://www.megauk.com/pcb_laminates.php, accessed September 2012

13 CST – Computer Simulation Tech. http://www.cst.com/, accessed 2012

14 Lamensdorf, D., Susman, L.: 'Baseband-pulse-antenna techniques', *IEEE Antennas Propag. Mag.*, 1994, **36**, pp. 20–30

15 Costa, J.R., Medeiros, C.R., Fernandes, C.A.: 'Performance of a crossed exponentially tapered slot antenna for UWB systems', *IEEE Trans. Antennas Propag.*, 2009, **57**, pp. 1345–1352

16 Mao, G., Fidan, B.: 'Localization algorithms and strategies for wireless sensor network' (Information Science Reference, 2009)

17 www.skycross.com, accessed September 2012

18 http://www.timedomain.com/p400.php, accessed September 2012

Q3

MAP20130245

Author Queries

Andela Zaric, Valter S. Matos, Jorge R. Costa, Carlos A. Fernandes

Q1   Please check the inserted main caption for Fig. 2.

Q2   As per journal style, colour figures are not allowed. Please change it to black & white.

Q3   Please add two more author names in Ref. [7] as per journal style.